©2017 Published in 5th International Symposium on Innovative Technologies in Engineering and Science 29-30 September 2017 (ISITES2017 Baku - Azerbaijan)

Characterization of Ion Substituted Calcium Phosphate Apatites Produced via Sol-Gel Method

[1]Ahmet TÜRK, [1]Fatih SARGIN
[1*]Faculty of Engineering, Department of Metallurgical and Materials Engineering, Manisa Celal Bayar University, Turkey

Abstract

Hydroxyapatite (HA) is one of the most popular biomaterial which has a wide variety of applications. Although HA biomaterials superior properties, dissolution behavior and implant stability properties of HA needs to be improved. One of the promising solution for these problems is incorporating Flourine (F) and Zinc (Zn) ions into HA structure. Sol-gel technique which has an effortless process control procedure, emerged as an ideal candidate for producing ion doped HA powders. Pure, F and Zn substituted HA powders obtained through sol-gel technique and SEM, EDX, XRD and FTIR analysis were performed. Results showed that F and Zn substitution into HA lattice was successful.
Key words: Hydroxyapatite, Ion Substitution, Sol-Gel

1. Introduction

Hydroxyapatite (HA), $Ca_{10}(PO_4)_6(OH)_2$ is one of the most known calcium phosphates that has numerous field of applications as implant or coating material. Some of the known applications of HA are bone fillers, biocompatible scaffolds [1], tissue repairing [2], and drug delivery systems [3]. Besides its excellent bioactivity, osteoconductive properties, chemical component and mechanical properties of HA shows great similarity with human bone. Synthetic HA has a Ca/P stoichiometric ratio of 1.67 and exhibits a special hexagonal crystal structure that has a P63/m space group [4-(Koutsopoulos, 2002]. Unlike synthetic HA, biologic apatites can have different stoichiometric phases. Main reason of this situation was considered ion substitutions which changes chemical composition of apatites. One of the best example for this case is human bone mineral which consists of trace elements such as Na, Mg, Zn, Sr, K, F, Cl and Si [4]. During the substitution cations generally takes place of Ca^{+2} ions in the lattice, and anions replaces OH sites.

As coating material, HA has been coated onto titanium (Ti) implants and often used dental and orthopedic applications. This was due to improve implant stability properties and reducing the time which is necessary for implant-tissue osseintegration process [5]. Studies showed that HA coatings improved the osseointegration time and bonding ability of Ti implants [6]. But there were some properties in HA coatings which needs to be improved. There were two cases for HA coating systems. First case was about the coating which has low dissolution property and remains stable during the implantation period and perform as a stable bioactive interface between implant material and tissue. Second case was about coatings which is almost temporary and has a high dissolution rate. In this case coatings were prompting fast bone tissue growth towards implant surface and in progress of time implant material bonds with tissue directly [7]. One must produce a thick coating in order to obtain stability and prevent direct contact of bone tissue with metallic implant surface.

*Ahmet TÜRK: Address: Faculty of Engineering, Department of Civil Metallurgy and Materials Engineering, Manisa Celal Bayar University, 45410, Manisa TURKEY. E-mail address: ahmet.turk@cbu.edu.tr, Phone: +902362012411

But with increasing coating thickness, possibility of coating delamination also increases.

Plasma spraying known as one of the most popular method for producing HA coatings. Also there are various other methods like magnetron sputtering, electro chemical deposition, pulsed laser deposition and sol-gel technique. Sol-gel method differs from other methods with the privilege of producing both HA coating and HA powder. Also, sol-gel technique provides chemical purity and low temperature during producing of coating or obtaining powder material. More over sol-gel technique is suitable for producing HA with ion substitution.

Ion substitutions in HA emerged as one of the promising approach for improving dissolution behavior and osseintegration process. Fluoridated hydroxyapatite (FHA) is one of the approach for improving dissolution resistance of HA [8]. FHA was considered too has a biocompatibility as much as HA. Therefore, application of thinner coatings of FHA, can solve the delamination problem that can be seen in thick coatings. When the risk of delamination decreases, coating life span increases which is the key feature for coating stability [6]. Another approach for HA coatings is improving osseintegration process time with ion substitution. One way to increase osseintegration is promote bone cells to settle on the implant surface and make strong bonding with the implant material. Zinc emerged as one of the promising candidate which has a prompting effect on bone tissue formation and osteoblast activity [10]. Studies revealed that releasing of Zn ions has a positive effect on bone formation on implant material surface [11].

In this study, ion substituted HA powders produced via sol-gel technique. For ion substitution F- and Zn+2 were chosen in order to obtain a powder mixture which is capable of both reducing dissolution rate and improving bone formation behavior.

2. Materials and Method

In order to produce pure HA powders with sol-gel technique calcium nitrate tetra hydrate ($Ca(NO_3)_2.4H_2O$) used as Ca source, di-ammonium hydrogen phosphate ($(NH_4)_2HPO_4$) used as P source and ammonium hydroxide (NH_4OH) used for adjusting pH value. The composition ratio of Ca/P adjusted 1.67. $Ca(NO_3)_2.4H_2O$ and $(NH_4)_2HPO_4$ dissolved in distilled water in separate container. Both solutions stirred vigorously for 2 hours and added NH_4OH for adjusting pH value between 11-12. After that $Ca(NO_3)_2.4H_2O$ solution added into the $(NH_4)_2HPO_4$ solution with a rate of 5ml/min. After that, solution take a milk-white color and stirred for 2 hours. After this step solution heated to 90°C and kept stirred for 1 hour. With the end of the stirring process solution aged in room temperature for 24 hours. After aging process solution filtered and dried in 70°C for 3 hours. After the drying, HA powders heat treated in 1000°C for 3 hours. For producing F^- substituted HA powder, ammonium fluoride (NH_4F) added in to P source with a P/F ratio of 4. And for producing Zn^{+2} substituted HA powders zinc nitrate hexahydrate ($Zn(NO_3)_2.6H_2O$) was added into Ca source with a Ca/Zn ratio of 10. Other steps were same for preparation of substituted HA powders.

Scanning electron microscopy (Carl Zeiss 300VP SEM) analysis were performed for HA powders produced via sol-gel technique in order to observe powder morphology and chemical compound. For chemical characterization X-Ray Diffracion analysis (PANalytical Empyrean X-Ray Difractometer) were performed with a Cu Kα.

Fourier Transformed InfaRed Spectrometer (FTIR) analyis were performed with Agilent Cary 660. Analysis were carried out for both doped and undoped HA powders with a wavenumber range of 400–4000 cm^{-1}.

3. Results

3.1 SEM Analysis

SEM images obtained for all powders and chemical analysis were performed based on that images. Figure 1 shows the SEM image and chemical analysis of pure HA. As can be seen in Figure 1, pure HA powders formed a cluster like scattered formation. Chemical analysis revealed that there is no element other than Ca, P and O which are the main components of pure HA.

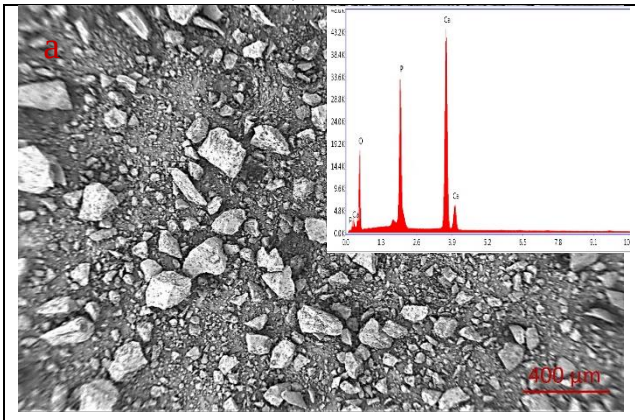

b)

Element	Weight %	Atomic %
O K	42.29	62.84
P K	16.83	12.92
Ca K	40.88	24.25

Figure 1. a) SE images and EDX spectrum of the precipitated and sintered pure HA **b)** EDX results of same sample

Figure 2 shows the SEM image and chemical analysis of F substituted HA.

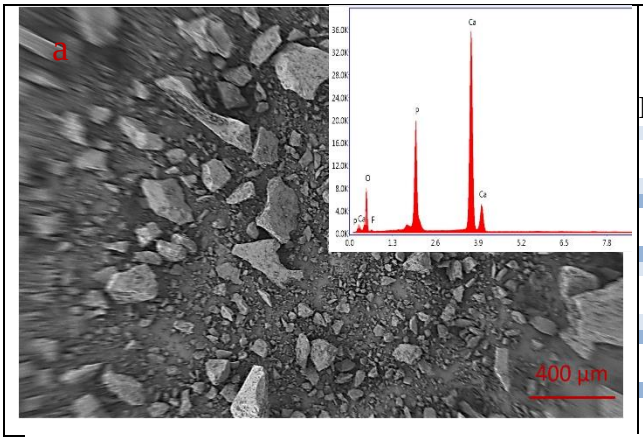

b

Element	Weight %	Atomic %
O K	32.89	52.61
F K	2.45	3.31
P K	14.94	12.34
Ca K	49.72	31.75

Figure 2. a) SE images and EDX spectrum of the precipitated and sintered F substituted HA **b)** EDX results of same sample

Figure 2 showed that F doped HA powders formed a cluster like scattered formation same as pure HA powders. Chemical analysis proved the existence of F beside Ca, P and O elements.
Figure 3 shows the SEM image and chemical analysis of Zn substituted HA.

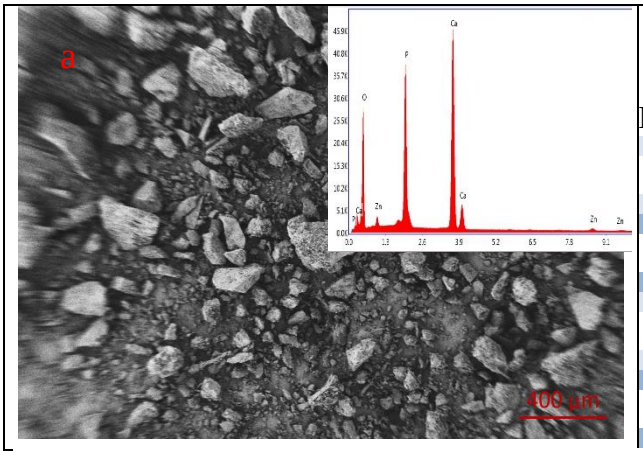

b

Element	Weight %	Atomic %
O K	48.03	68.31
P K	15.76	11.58
Ca K	34.17	19.40
Zn K	2.04	0.71

Figure 3. a) SE images and EDX spectrum of the precipitated and sintered Zn substituted HA **b)** EDX results of same sample

Figure 3 showed that Zn doped HA powders formed a cluster like scattered formation same as pure HA and F doped HA powders. Chemical analysis proved the existence of Zn beside Ca, P and O elements.

3.2 XRD Analysis

XRD analysis were performed with a range of 20 to 60 2θ degrees. Figure 4 shows the XRD patterns of heat treated pure HA, F^- substituted HA and Zn^{+2} substituted HA powders.

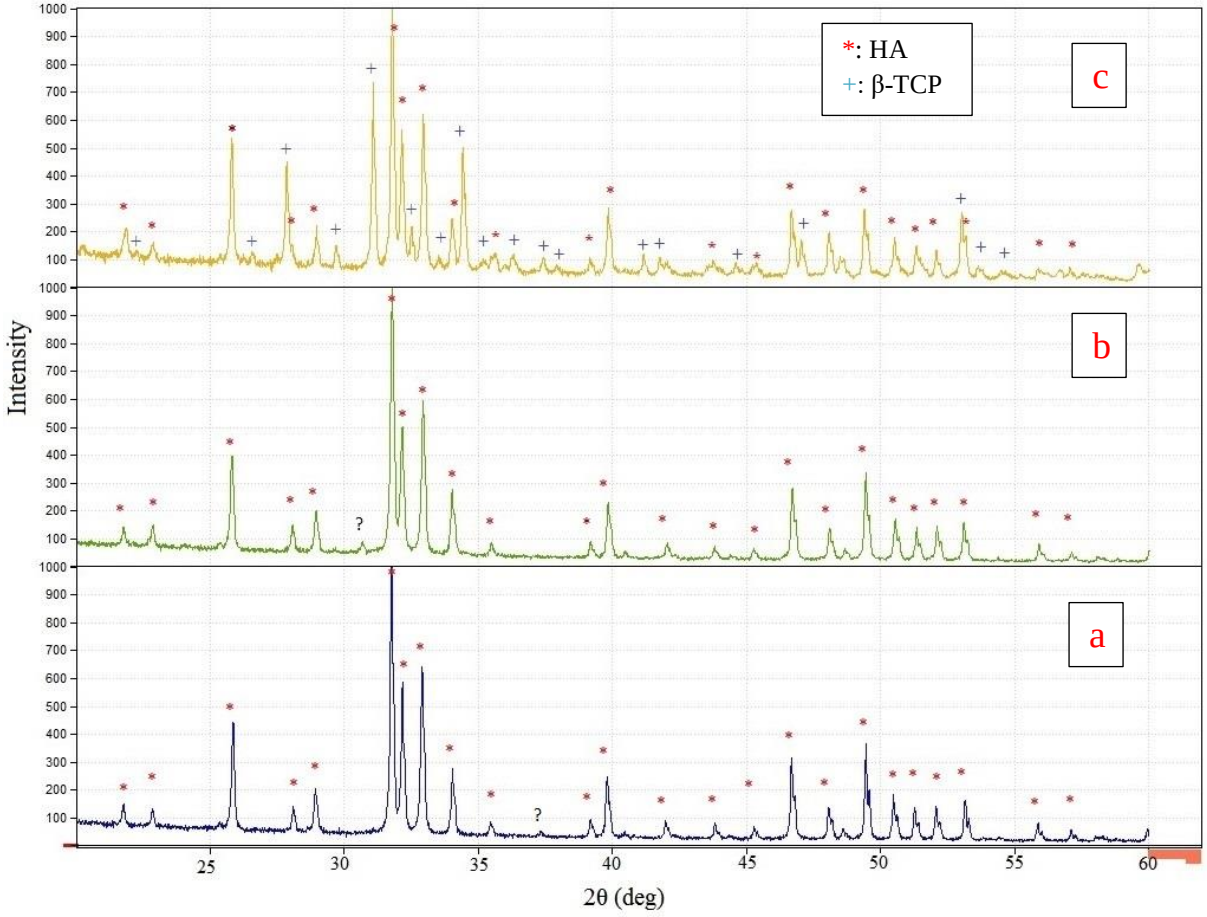

Figure 4. XRD patterns of heat treated **a)** pure HA **b)** F substituted HA and **c)** Zn substituted HA powders.

As can be seen in the XRD patterns, because of the annealing process at 1000°C, all powders showed a crystalline phase. Pure HA and F- doped HA powder patterns exhibit only HA phase, while Zn+2 doped HA powder patterns show both HA and β-Tri Calcium Phosphate (β-TCP). It is also clear that in Zn+2 doped HA powder, ratio of HA phase is higher than β-TCP phase. Peaks at 25.79, 31.78, 32.14 and 32.93 degrees which corresponds to lattice parameters (002), (121), (112) and (300) indicates the presence of HA phase. And peaks at 27.84, 31.07 and 34.42 degrees which corresponds to (214), (0210) and (220) reflections indicates the presence of β-TCP phase

3.3 FTIR Analysis

In order to confirm ion substitution in the HA structure, pure HA and ion substituted HA powders, FTIR analysis were performed. Figure 5 shows the FTIR spectra of annealed pure HA powder. FTIR measurements showed peaks around 550-630 cm^{-1} and 900-1100 cm^{-1}. Also another observable peak detected around 3570 cm^{-1}.

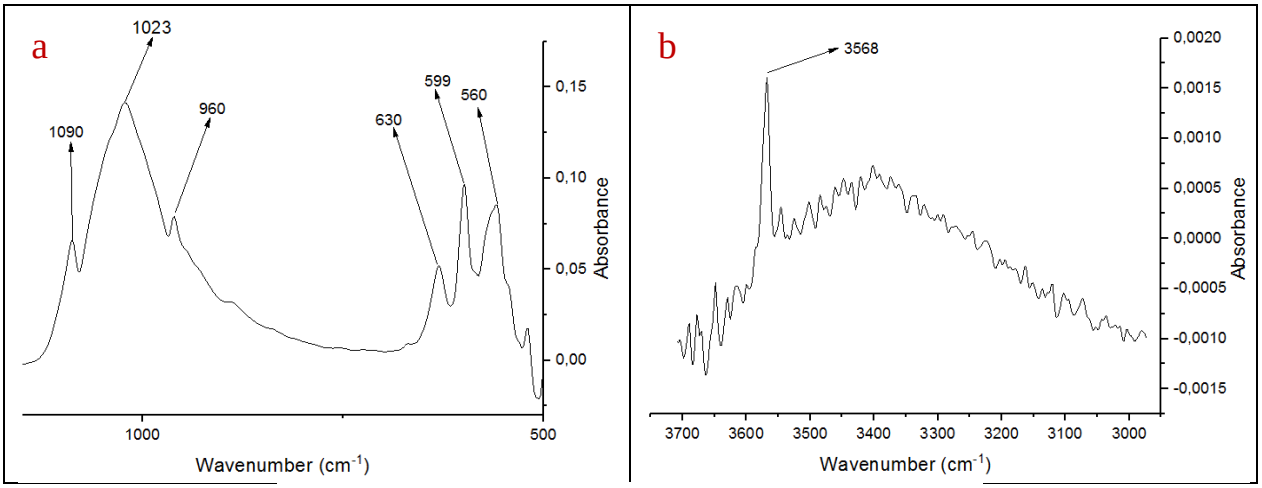

Figure 5. a) and **b)** FTIR spectra of heat treated pure HA powder.

Figure 6 shows FTIR spectra of heat treated F substituted HA powder. As can be seen in Figure 6, new peaks appeared at 674 and 720 cm^{-1} while the peak around 630 cm^{-1} disappeared. In addition to that 960 and 3568 cm^{-1} peaks which was clear in pure HA powder shifted to new positions as 964 and 3543 cm^{-1}.

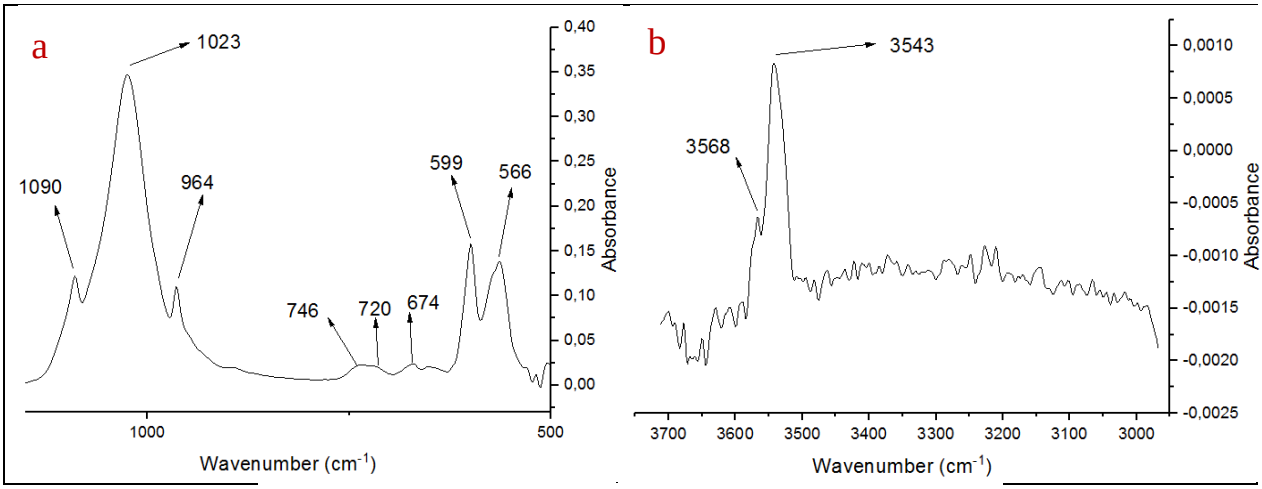

Figure 6. a) and **b)** FTIR spectra of heat treated F doped HA powder.

Figure 7 shows FTIR spectra of annealed Zn substituted HA powder. It can be seen in Figure 7.a that pure HA powder peaks shifted to 1087,1022 cm^{-1} and peak at 960 cm^{-1} decreased and shifted to 964 cm^{-1}. Also pure HA peak at 560 cm^{-1} decreased and broadened. Another difference with HA powder was observed peak at 3569 cm-1 , as the peak in Zn substituted HA powder shifted to 3570 cm^{-1} position. Also a new peak emerged at 3407 cm^{-1} position which can be seen in Figure 7. b.

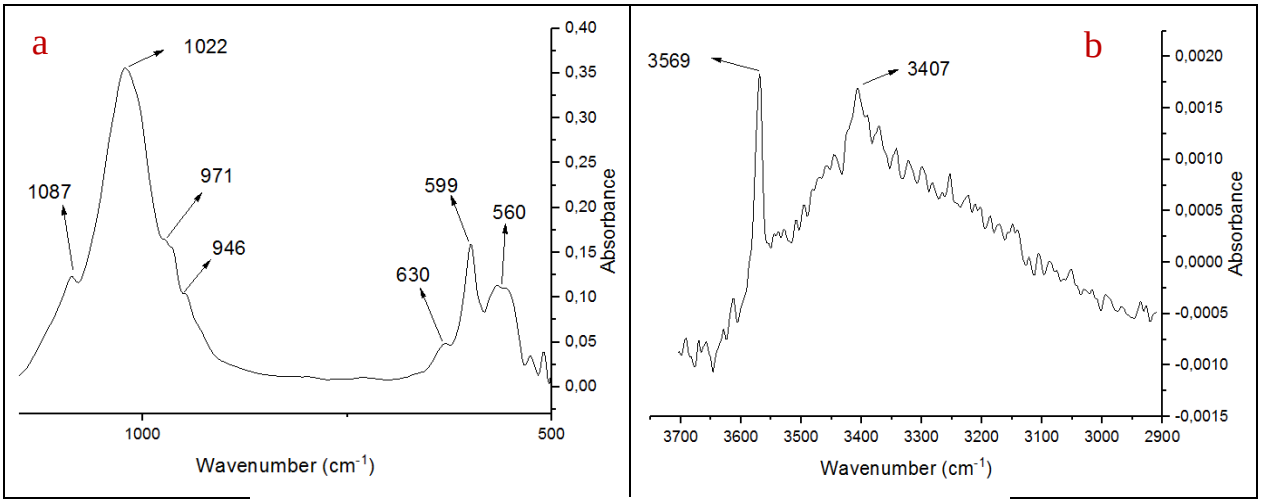

Figure 7. a) and **b)** FTIR spectra of heat treated Zn doped HA powder.

4. Discussion

HA powder morphology is one of the important properties in determining the microstructural formation of HA ceramics which effects the biological, physical and mechanical properties of implant materials [12]. As can be seen in Figure 1.a, Figure 2.a) and Figure 3.a, all of the HA powders formed a cluster like scattered formation that have different powder sizes. The powders look like to be of crushed angular shape and images revealed that bigger HA particles are consisted of agglomerated fine particles. This results showed that the annealing temperature which was used in this study is enough to sinter these agglomerated particles. The EDX spectrum of pure HA powder shown in Figure 1.b, showed existence of Ca, P and O elements. In Figure 2.b, in addition to Ca, P, and O, existence of F element detected with a molar ratio of %3.31, as expected. And Figure 3.b showed that addition to Ca, P and O, Zn element was observable with a molar ratio of %0.71. Ca/P ratios showed difference for all powders. This phenomenon attributed to non-homogenous particle distribution. Interestingly only Zn doped HA powders showed Ca/P ratio of 1.67.

XRD patterns of heat treated HA powders are shown in Figure 4. As can be seen pure HA and ion substituted HA powders show high intensity which is a sign of high crystallinity. There were no other phases detected from HA and TCP, according to XRD patterns. Kuriakose, T. Anee, et al. produced HA powder via sol-gel technique and sintered product at different temperatures [13]. They confirmed that, as dried powders showed low rate intensity and powders that sintered at higher temperatures showed higher intensity which is also concluded as evidence of higher crystallization rate. Pure HA powder spectra in Figure 4.a showed all the characteristic peaks of HA structure with an unknown peak around 37 degrees. Kurtz, S. M. [14] observed same peak in HA structure and identified it as a result of CaO phase with a very low rate. Chew, WJ Kelvin, et al. [12] revealed that HA powders obtained via sol-gel technique shows decomposition of HA above 1200°C. Because of that CaO phase which identified in pure HA powder must be product or

remnant of sol-gel process. Figure 4.B show the spectra of F doped HA powders and it is almost same with pure HA powder XRD patterns. Miao, Shundong, et al.[11] sintered F doped HA powders at 600° C and obtained an XRD pattern which has only HA formation with high crystallinity. Previous studies showed that after the heat treatment of F containing HA powders at 800°C, a small amount of β-TCP phase could be observed which a product of decomposition is of HA. XRD spectra in Figure 4.b showed a small peak around 31 degrees which is identified by Kurtz, S. M. [14] as the existence of small amount β-TCP phase. Figure 4.c shows the XRD pattern of Z doped HA powders which actually consist of HA and β-TCP phases. Norhidayu, D. et al. [15] proved that XRD patterns of Zn doped powders that calcined at 700 and 800°C showed TCP phase. Also it was noted that with the increasing calcination temperature concentration of TCP phase increased. Xiao, Xiufeng, et al. [16] stated that after heat treatment at 800°C, Zn doped HA powders transformed into Zn doped β-TCP powders. Also it was observed that with the increasing Zn fraction, β-TCP phase peaks increased. Thus it was concluded that with the increasing amount of Zn incorporated to lattice, thermal stability of Zn doped HA powder decreases. As can be seen in Figure 4.c, in our study Zn doped HA powders that was heat treated at 1000°C showed TCP phase which was agreeable with the literature. It can be said that high heat treatment temperature resulted with high TCP phase concentration.

XRD analysis revealed that the all samples are consisted of HA and/or TCP phases. In order to confirm that F and Zn incorporation into the apatite structure, FTIR analysis needs to be performed. FTIR spectra which is obtained from pure HA powders shown in Figure 5. Lala, S., et al.[17] analyzed undoped HA powder with FTIR and our results were agreeable with that study. In our study Figure 5 revealed, typical v3 asymmetric P-O stretching mode at 1090 and 1023 cm^{-1}, v1 symmetric P-O stretching mode at 960 cm^{-1}, and O-P-O bending mode v4 at 560 and 599 cm^{-1}. In addition to that O-H bending peak at 630 cm^{-1} and O-H stretching peak at 3568cm^{-1} are characteristic peaks for stoichiometric HA [13]. No other peaks observed in FTIR analysis for pure HA powder. Figure 6 shows the FTIR spectra of F doped HA powder which has a few differences from HA powder. Firstly, peaks at P-O peaks at 1090, 1023, and 599 cm^{-1} are same as pure HA, and at 964 and 566 cm^{-1} showed a small shift. In addition to that, with the incorporation of F to HA lattice, O-H peak which was in 630cm^{-1} disappeared and a new peaks appeared at 674cm^{-1} and between 720 and 746 cm^{-1}, also peak at 3568cm^{-1} decreased and a new peak emerged because of OH-F stretching at 3543cm^{-1} which is similar with the studies made by Zhang, Sam, et al.[18] and Wang, Jian, et al.[19]. When OH- was partially replaced with F- ions, OH-F stretching bands appeared in the spectrum [19]. Figure 7 shows the FTIR spectra of Zn doped HA powders which has similarities with pure HA powder. P-O stretching peaks at 1022 and 1087cm^{-1} shifted very little and 599cm^{-1} peak remained same position according to pure HA powder spectra in Figure 6.A. With the incorporation of Zn, O-H bending peak at 630cm^{-1} and P-O stretching peak around 960 cm^{-1} decreased and broadened as a sign of decrease in crystallization which agree with results of XRD patterns in Figure 4 [18]. As the peak at 960 cm^{-1} decreased, new slight P-O peaks appeared at 946 and 971 cm^{-1} as a sign of β-TCP existence which is similar with the previous studies in the literature [20] Also as can be seen in Figure 8.b O-H stretching peak at3569cm^{-1} remained same but a new O-H peak emerged at 3407 cm^{-1} as a result of Zn incorporation which is also supported by the studies in literature [20, 21].

Conclusions

Pure HA and ion doped HA powders successfully produced by sol-gel technique. SEM analysis revealed that all the powders showed an angular shape that consist highly agglomerated nano particles as an effect of high annealing temperature and had different Ca/P ratios. According to EDX analysis Zn, F elements were found in substituted HA samples and XRD analysis revealed that Zn and F ions are in the HA crystal structure because of these elements were not observed in the XRD spectra. Although EDX analysis proved Zn and F content in doped HA powders, XRD analysis showed that undoped and F doped HA powders consist only crystalline HA phase while Zn doped HA powder has both HA and β-TCP phase as expected. No other phases detected that includes F or Zn. FTIR analysis confirmed that F and Zn ions incorporated to HA and β-TCP lattice structure as a sign of successful element doping procedure.

Acknowledgements

This study supported by Manisa Celal Bayar University Scientific Committee Project 2016-037.

References

[1] Dorozhkin, S., Materials 2, Calcium orthophosphate cements and concretes. 2009, 221–291.
[2] Liu, M. et al., Effect of nano-hydroxyapatite on the axonal guidance growth of rat cortical neurons. Nanoscale 4, 2012, 3201–3207
[3] Li, J., Chen, Y.C., Tseng, Y.C., Mozumdar, S., Huang, L., Biodegradable calcium phosphate nanoparticle with lipid coating for systemic siRNA delivery. J. Control. Release, 2010, 142, 416–421.
[4] Lin, K. et al., Biomimetic hydroxyapatite porous microspheres with co-substituted essential trace elements: surfactant-free hydrothermal synthesis, enhanced degradation and drug release. J. Mater. Chem. 21, 2011, 16558–16565.
[5] Albrektsson T, Branemark PI, Hansson HA, Lindstrom J. Osseointegrated titanium implants. Requirements for ensuring a long-lasting, direct bone-to-implant anchorage in man. Acta Ortho Scand 1981;52:155–70
[6] McPherson EJ, Dorr LD, Gruen TA, Saberi MT. Hydroxyapatite-coated proximal ingrowth femoral stems.matched pair control study. Clinical Orthopaedics and Related Research 1995:223–30.
[7] Tredwin, Christopher J., et al. Hydroxyapatite, fluor-hydroxyapatite and fluorapatite produced via the sol–gel method: bonding to titanium and scanning electron microscopy. Dental Materials, 2013, 29.5: 521-529.
[8] K. Cheng, S. Zhang, W. Weng, and X. Zeng, The Interfacial Study of Sol– Gel-Derived

Fluoridated Hydroxyapatite Coatings, Surf. Coat. Technol., 198,242–6 (2005).
[9] G. Willmann, Coating of Implants with Hydroxyapatite Material Connections Between Bone and Metal, Adv. Eng. Mater. 2, 1995, 95–105.
[10] Grandjean-Laquerriere, Alexia, et al. Influence of the zinc concentration of sol–gel derived zinc substituted hydroxyapatite on cytokine production by human monocytes in vitro. Biomaterials, 2006, 27.17: 3195-3200.
[11] Miao, Shundong, et al. Zn-Releasing FHA Coating and Its Enhanced Osseointegration Ability. Journal of the American Ceramic Society, 2011, 94.1: 255-260.
[12] Chew, WJ Kelvin, et al., Influence of powder morphology and sintering temperature on the properties of hydroxyapatite. International Journal of Automotive and Mechanical Engineering 12, 2015: 3089.
[13] Kuriakose, T. Anee, et al. "Synthesis of stoichiometric nano crystalline hydroxyapatite by ethanol-based sol–gel technique at low temperature." Journal of Crystal Growth 263.1 (2004): 517-523.
[14] Kurtz, Steven M., ed. PEEK biomaterials handbook. William Andrew, 2011, Page:126
[15] Norhidayu, D.; Sopyan, I.; Ramesh, S. Development of zinc doped hydroxyapatite for bone implant applications. In: ICCBT 2008 Conference. 2008. p. 257-270
[16] Xiao, Xiufeng, et al. "Structural characterization of zinc-substituted hydroxyapatite prepared by hydrothermal method." Journal of materials science: Materials in medicine 19.2 (2008): 797-803.
[17] Lala, S., et al. "Structural and microstructural interpretations of Zn-doped biocompatible bone-like carbonated hydroxyapatite synthesized by mechanical alloying." Journal of Applied Crystallography 48.1 (2015): 138-148.
[18]Zhang, Sam, ed. Hydroxyapatite coatings for biomedical applications. CRC press, 2013, Page: 150-154
[19] Wang, Jian, et al. "Fluoridated hydroxyapatite coatings on titanium obtained by electrochemical deposition." Acta Biomaterialia 5.5, 2009: 1798-1807.
[20] Berzina-Cimdina, Liga, and Natalija Borodajenko. "Research of calcium phosphates using Fourier transform infrared spectroscopy." Infrared Spectroscopy-Materials Science, Engineering and Technology. InTech, 2012.APA
[21] Han, Jae-Kil, et al. "Synthesis of high purity nano-sized hydroxyapatite powder by microwave-hydrothermal method." Materials chemistry and physics 99.2, 2006: 235-239.